

Gravity selector-enabled kenaf recirculation and reuse as a renewable ballasting agent for sludge settleability enhancement in a municipal wastewater secondary process: A real wastewater pilot-scale study

Pranta Roy

Thesis submitted to the faculty of the Virginia Polytechnic Institute and State University in partial fulfillment of the requirement for the degree of

Master of Science

in

Biological Systems Engineering

Zhiwu Wang, Chair

Jingqiu Liao

Yiming Feng

December 17, 2024

Blacksburg, Virginia

Keywords: Ballasting; kenaf; settleability; OUR; SVI; zone settling velocity.

© Copyright 2024, Pranta Roy

Gravity selector-enabled kenaf recirculation and reuse as a renewable ballasting agent for sludge settleability enhancement in a municipal wastewater secondary process: A real wastewater pilot-scale study

Pranta Roy

ABSTRACT:

Sludge densification can be achieved either through granulation/densification, migrating carriers, ballasted flocculation, or a combination of these approaches. Hydrocyclone-enabled continuous flow densification has been applied for full-scale applications; however, it requires long startup times and, in some instances, results in poor stability of the densified floc. Migrating carriers hold promise to offset these disadvantages for continuous flow processes where a reasonable feast-famine or plug flow conditions cannot be achieved, while drawing on the strength of hydrocyclones to retain and return the ballasting agent. This idea was tested by dosing kenaf, a plant-based renewable migrating carrier in a pilot-scale plug flow reactor equipped with a gravity selector to mimic a hydrocyclone. Results showed that kenaf was able to gradually reduce the sludge volume index from 170 to 50 mL/g and increase zone settling velocity from 2.5 to 7 m/h over 110 days without compromising treatment performance. Because of the selective retention of the inert plant-based carrier represented as a volatile solid in the gravity selector underflow, a traditional SRT calculation based on mixed liquor volatile suspended solids tended to overestimate daily Waste Activated Sludge (WAS) requirements and resulted in active sludge inventory loss. An oxygen utilization rate-based method was developed and verified for easy SRT correction to avoid kenaf interference with the sludge wasting protocol. Denser kenaf incorporated into the sludge matrix during flocculant settling contributed to the settleability improvements. However,

a lack of biofilm formation on the kenaf surface was observed even after 110 days of treatment is intriguing and different from other studies. Challenges with initial kenaf floating and interference with conventional SRT calculations were two significant lessons learned from this study, and countermeasures were provided accordingly. It was concluded that kenaf can work in synergy with gravimetric ballast separation, such as with a hydrocyclone, for quick and sustainable sludge settleability improvements.

Gravity selector-enabled kenaf recirculation and reuse as a renewable ballasting agent for sludge settleability enhancement in a municipal wastewater secondary process: A real wastewater pilot-scale study

Pranta Roy

GENERAL AUDIENCE ABSTRACT:

Improving wastewater treatment involves making the sludge (the solid part of the waste) settle faster and more efficiently. This can be done in two main ways, i.e. forming dense, compact sludge particles or using materials to make the particles heavier so they settle quicker. A trendy method, known as "aerobic granulation," uses special equipment but has drawbacks, i.e., it takes a long time to get started, and the particles aren't very stable. Another method, "ballasted flocculation," shows promise because it can address these issues while still using the same equipment for reusing the added material. To test this hypothesis, we investigated using a natural material called kenaf, a plant-based product, to help improve sludge settling. We ran the experiment in a small-scale treatment system designed to mimic large-scale operations. Adding kenaf reduced the volume of sludge by over two-thirds and made it settle three times faster, and all these were achieved without affecting the wastewater treatment performance. However, using kenaf introduced some challenges. It made it harder to accurately measure how much sludge was being wasted daily, leading to an unexpected loss of sludge in the system. To fix this, we developed a novel, simple method to calculate sludge levels more accurately. We also found that kenaf worked well because it became part of the sludge, helping it settle faster, though it didn't let bacteria grow on its surface. Two key lessons emerged, and we suggested ways to deal with these problems. Overall, kenaf worked effectively with existing equipment to make sludge settle faster and more sustainably, offering a promising solution for wastewater treatment systems.

DEDICATION

This thesis is dedicated to my parents, Beena and Nitai Roy, and to my elder brother Partha Roy.

Thank you!

ACKNOWLEDGEMENTS

I would like to express my sincere gratitude to the following people for their time, guidance, and efforts throughout this research project.

My advisory committee:

Dr. Zhiwu Wang, committee chair and advisor, for the research opportunity and for teaching me how to ‘think like an engineer’.

Dr. Jingqiu Liao, for research advice and support.

Dr. Yiming Feng, for research review and recommendations.

NEWhub Water Corporation, Herndon, Virginia, USA:

Dr. Sudhir Murthy, for providing the study concepts, design, and reviewing the results.

Upper Occoquan Service Authority (UOSA):

Matt Brooks, for assistance with methods and setup of experimental design and reactor setup.

Bob Angelotti, for assistance with the sponsorship to do the study.

Nuvoda, Raleigh, North Carolina, USA:

Mr. Jason Calhoun, for providing kenaf used in this research.

The Occoquan Watershed Monitoring Laboratory (OWML):

In particular,

Dongmei Alvi, Missy Alison, Cathy Sledz, and Curt Eskridge.

TABLE OF CONTENTS

CHAPTER 1: INTRODUCTION.....	1
1.1 Background.....	1
1.2 Research Goal.....	4
1.3 Research objective.....	4
CHAPTER 2: MATERIALS AND METHODS	6
2.1 Reactor design and operation.....	6
2.2 Analytical methods.....	9
2.3 Particle size and image analysis methods.....	10
2.4 Kenaf settling velocity.....	10
2.5 Kenaf concentration calibration.....	11
2.6 Confocal microscopy visualization of kenaf surface.....	14
CHAPTER 3: RESULTS	15
3.1 Sludge settleability before and after kenaf addition.....	15
3.2 Treatment performance before and after kenaf addition.....	17
3.3 Effectiveness of the gravity selector in retaining and returning kenaf.....	20
3.4 Development of a novel SRT control method specifically tailored for using kenaf as a ballasting agent.....	24
3.5 Monitoring of kenaf settling in sludge blanket.....	26
3.6 Confocal microscopy visualization of the kenaf surface.....	29
CHAPTER 4: DISCUSSION	31
4.1 Mechanism of kenaf-enhanced sludge settleability.....	31
4.2 Lessons learned from this study.....	33
CHAPTER 5: CONCLUSIONS	35
REFERENCES.....	36

LIST OF FIGURES

Figure 1 (A) Schematic diagram and (B) photos of a 10-chamber PFR equipped with a gravity selector, a clarifier, and NRCY flow.	8
Figure 2 (A) Morphology of 10 pieces of kenaf particles randomly sampled from the pilot reactor, (B) Settling velocity v.s. particle size of the ten randomly collected kenaf particles.	11
Figure 3 (A) 500-mesh sieve; (B) Kenaf particle separated from 250 mL mixed liquor using sieve; (C) rinsed kenaf body transferred to a petri dish; (D) Kenaf sample transferred into an aluminum dish for dry mass measurement in an oven; (E) Image of a 10 mL mixed liquor sample in a petri dish; (F) Petri dish image processed with bandpass filter using ImageJ 2.0; (G) Identified kenaf particle in the petri dish by ImageJ 2.0; (H) Outline image of kenaf particle available in the petri dish sample, and (I) Correlation between kenaf dry mass concentration and surface area projection in petri dish normalized to the sample volume.	13
Figure 4 Profiles of (A) SVI and (B) zone setline velocity before and after kenaf addition; (C) Settled sludge volume ratios measured at various MLSS; (D) An image of kenaf particles (white) mingled within the sludge blanket observed during SVI test after 30 min settling.	17
Figure 5 Removal efficiencies and effluent concentrations of (A) sCOD, (B) $\text{NH}_4^+\text{-N}$, and (C) TIN before and after kenaf addition, (D) $\text{NO}_3^-\text{-N}$ influent and effluent concentration profiles before and after kenaf addition, (E) TSS & VSS concentration of gravity selector underflow, and (F) TSS & VSS concentration of return activated sludge.	19
Figure 6 (A) Fractions of kenaf and activated sludge partitioned into the underflow at different ratios of underflow rate-to-total return flow rate which is also indicated by the blue line; (B) Particle size distribution profile determined by particle size analyzer for underflow and overflow grabbed samples before and after kenaf addition. The box-whisker plot was used in which average particle size was indicated by \times symbol with upper and lower whisker boundary of 1.5 Interquartile range (IQR); (C) Fractions of heterotrophs and nitrifiers partitioned into the underflow; and (D) The biomass contents of activated sludge in gravity selector inflow and overflow.	23

Figure 7 (A) MLSS and MLVSS concentrations measured in Chamber 10; (B) WAS flowrate calculated based on SRT using MLSS in Eq. 1 and MCRT using OUR in Eq. 6, respectively. .. 26

Figure 8 (A) The setup of a column settling test that allows samples to be taken at various heights of a column; (B) Petri dish images of samples taken from different column heights at various sampling time, (C) Kenaf surface area present in unit volume of samples, and (D) Kenaf mean sizes measured at the different settling time and height of the column. 28

Figure 9 Confocal microscopy visualization of the (A) auto-fluorescent image of kenaf surface, and (B) bacterial cells scattered on kenaf surface. Sample was taken 105 days after kenaf addition. 30

Figure 10 Schematic illustration of the mechanism of kenaf-enhanced sludge settleability. 32

Figure 11 (A) Kenaf floating on the mixed liquor surface; (B) Water level difference caused by tubing clogging between chambers; (C) Tubing being clogged by kenaf; (D) Kenaf clogging tubing connectors. 34

LIST OF TABLE

Table 1 Kenaf media specification	9
--	---

CHAPTER 1: INTRODUCTION

1.1 Background

Ballasted flocculation is a method that has been used for decades to improve the settling of suspended particles in the treatment of drinking water (Sang et al., 2022), stormwater (Kumar et al., 2019), and wastewater (Sang et al., 2022) including the activated sludge system (Chhuon et al., 2020; Ma et al., 2023). In recent years, a plant-based material such as kenaf has been used as a renewable migrating carrier of low degradability for sludge densification in secondary wastewater treatment (Boltz and Daigger, 2022). However, because such plant derived material (including kenaf, hemp, etc.) is mingled with Waste Activated Sludge (WAS), its continuous loss through daily WAS discharge requires continuous supplementation of new kenaf unless an effective kenaf separation and recovery system is in place. Moreover, whether the occupation of activated sludge inventory by the inactive kenaf may compromise the treatment performance is also in question.

This study utilized a ballasting agent derived from kenaf, a lignocellulosic material characterized by its components: cellulose, hemicellulose, and lignin. The hydrophilic properties of cellulose and hemicellulose enable efficient water uptake, whereas lignin's hydrophobic nature minimizes water loss and reinforces the plant's structural stability.

Scientifically, cellulose is a carbohydrate polymer consisting of glucose units connected through $\beta(1\rightarrow4)$ glycosidic bonds, forming extended chains. Its structure is highly hydrophilic because it

has numerous hydroxyl (-OH) groups that attract water molecules. Hemicellulose, although structurally different from cellulose, is also hydrophilic. It consists of a variety of sugar monomers, such as xylose, arabinose, glucose, mannose, and galactose, which enhance its ability to interact with water. Lignin, in contrast, is rich in aromatic subunits, making it hydrophobic and water-resistant. Its primary function is to provide support and regulate water transport within the plant stem.

When kenaf is processed into tiny particles, the lignin barrier breaks down, mingling with cellulose and hemicellulose. This disruption exposes the hydrophilic properties of cellulose and hemicellulose, making the overall surface of kenaf hydrophilic. Additionally, lignocellulosic materials are hygroscopic, further emphasizing their water-attracting nature (Rodriguez-Fabia et al., 2022).

Currently, the most popular sludge densification technology being deployed for continuous flow Wastewater Resource Recovery Facilities (WRRFs) is the hydrocyclone-enabled sludge densification, a type of activated sludge densification suited to these continuous flow applications (Bauhs et al., 2024). This technology offers several advantages that have gained acceptance in the wastewater industry. It improves sludge settleability and reduces the sludge volume index (SVI) by exerting selection pressure through a hydrocyclone to selectively return larger, denser sludge particles retained in the underflow and reject lighter, smaller sludge particles through the overflow (Regmi et al., 2022). This technology does not need major infrastructure modifications and thus can be easily adopted by existing WRRFs (Avila et al., 2021). However, there are two major challenges with hydrocyclone-enabled sludge densification, namely long lead times to achieve the

desired settleability improvement and relatively low stability of the densest sludge particles at plants where plug flow characteristics are not easily achievable due to large mixed liquor recirculation rates. The startup optimization for densification to enable biological selection of dense sludge, such as including the promotion of feast famine regimes can prolong a startup. Due to the slowness of biological processes, it may take half a year for aerobic granular sludge to be formed and the sludge densification to be achieved (Ford et al., 2016; Franca et al., 2018; Kent et al., 2018; Welling et al., 2015; Wett et al., 2015). Moreover, the structural stability of aerobic granular sludge that is formed under poor biological selection pressure has been a concern at facilities where feast-famine selection regimes are not easily achieved. Mysterious disintegration of the aerobic granular sludge for no obvious reasons has been reported (Franca et al., 2018; Lee et al., 2010). Therefore, caution must be taken toward complete reliance on aerobic granular sludge for sludge densification in the continuous flow secondary wastewater treatment. At minimum, a rescue measure should be in place to handle the emergency of accidental sludge settleability loss.

One advantage of ballasted flocculation over aerobic granular sludge is its immediate effect on sludge densification because ballasted flocculation is more or less a physical process (Roche et al., 2022). For this reason, great interest has been shown towards ballasted flocculation for its large treatment capacity with a small footprint requirement (Gasperi et al., 2012). Moreover, plant-based material such as kenaf's affordability, availability, and ease of storage and transportation enhance its suitability as a ballasting agent to address the challenges associated with hydrocyclone-enabled continuous flow aerobic granulation, such as long startup time and accidental sludge settleability losses.

1.2 Research Goal

While prior studies employed rotary screens to separate kenaf particles from the WAS (Wei et al., 2021), the possibility of taking advantage of the existing hydrocyclone to separate kenaf particles from the WAS has not been explored. Therefore, there is an opportunity to dose kenaf into hydrocyclone-installed secondary wastewater treatment process to achieve quick sludge settleability improvement and multiple cycles of kenaf reuse from a single addition. This novel integration of kenaf with hydrocyclone has not been explored before. So, the goal of this study is to check the feasibility of taking advantage of the existing hydrocyclone to separate kenaf particles from the WAS.

1.3 Research objective

This study investigates the impact of kenaf addition on sludge settleability and treatment performance. Since the hydraulic selection pressure provided by hydrocyclones can be mimicked by gravity selectors (An et al., 2023), the objectives of this study are to:

- 1) determine whether dosing kenaf can quickly increase sludge settleability while safeguarding the effluent quality in a gravity selector-installed Modified Ludzack Ettinger (MLE) secondary treatment system;
- 2) investigate the efficiency of a gravity selector in separating and returning kenaf particles; and
- 3) understand the mechanistic and operational difference between kenaf and aerobic granular sludge in the hydrocyclone-enabled sludge densification system. The outcome from this study is expected to provide fundamental understanding and engineering guidance for researchers and engineers considering drawing on the strengths and offset the weaknesses of hydrocyclone- and

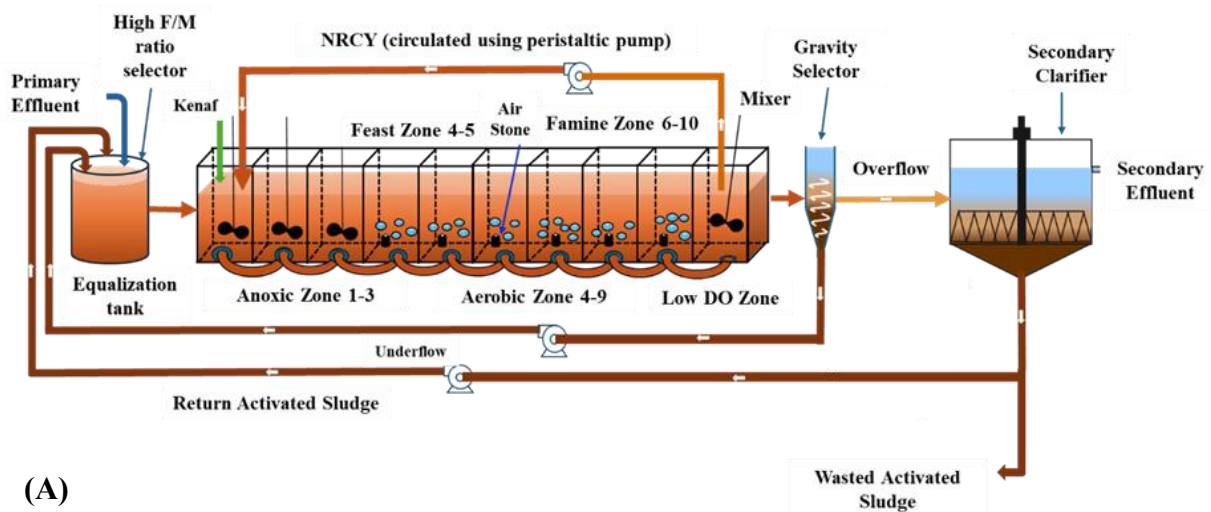
ballasted flocculation- enabled sludge densification through a synergistic integration of the two technologies.

CHAPTER 2: MATERIALS AND METHODS

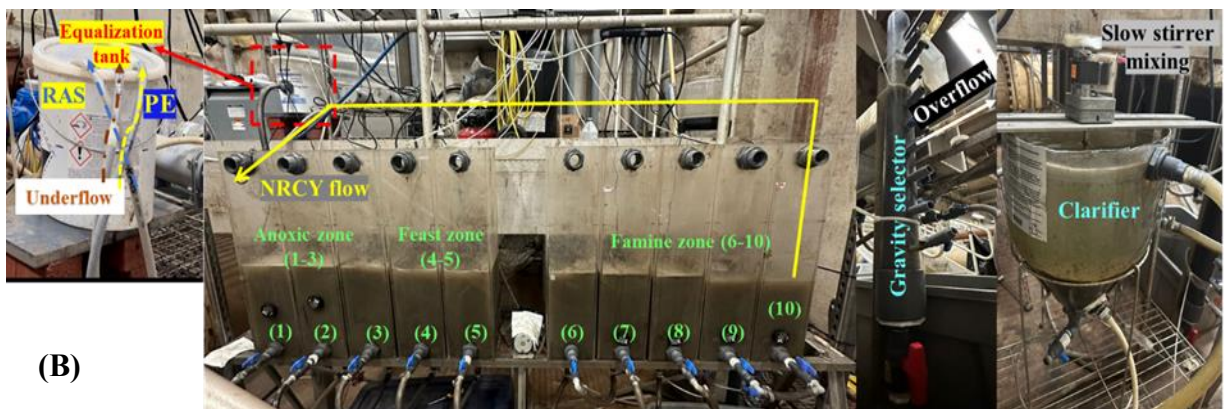
2.1 Reactor design and operation

The pilot-scale plug flow reactor (PFR) used in this study is illustrated in Figure 1A. The total working volume of the PFR was 150 L and operated on-site at Upper Occoquan Service Authority (UOSA), a WRRF located in Centreville, VA, USA. The pilot PFR setup was designed to mimic the full-scale MLE process being used at UOSA. The pilot reactor influent was fed continuously with UOSA primary effluent (PE), without additional pretreatment or conditioning. The PFR consists of 10 completely stirred tank reactors (CSTRs) in series with hydraulic retention time (HRT) controlled at 6.5 hours. The SRT of the system was controlled at 15 days throughout the study by WAS removal after sludge settling in the clarifier (Figure 1). As depicted in Figure 1A, the 10 CSTR chambers can be divided functionally into anoxic and aerobic zones. The first 2~3 chambers were designated as the anoxic zone and mixed with mechanical mixers (Danner Manufacturing, Inc., Supreme Aqua-Mag 1200 GPH Magnetic Drive Water Pumps). The remaining 6~7 chambers served as the aerobic zone and were mixed and aerated with aquarium type air stone diffusers located at the chamber bottom. Enough air was supplied to maintain dissolved oxygen (DO) levels between 0.5~2.0 mg/L depending on the cell location in the process. The last (10th) chamber was operated in a way to reduce DO residue in nitrate recycle (NRCY), i.e., only using a mechanical mixer to keep the sludge suspended. The NRCY:PE flow rate ratio was kept at 4:1 throughout the studies. Based on the chemical oxygen demand (COD) profile, chambers 4 and 5 can be regarded as the feast zone while chambers 6~10 can be regarded as the famine zone (Figure 1A).

An internal diameter of 5 cm and a total working height of 120 cm of a continuous upflow column was installed at the end of the PFR to mimic a high-rate clarifier according to a previous study (Sun et al., 2019). The column inflow, i.e., the mixed liquor from the PFR effluent, continuously entered at the height of 30 cm from the column bottom and then flowed up for 50 cm before overflowing from the top of the upflow column (Figure 1). The surface overflow rate (SOR) of this gravity selector column was set at 10~15 m/h to separate the sludge and kenaf particles based on their settling velocity. Theoretically, only those particles with a settling velocity greater than 10~15 m/h can be retained within the underflow of the gravity selector and returned to the equalization tank of the PFR (Figure 1). The flow rate ratio of selector overflow to underflow was set at about 2.3~3.5. The unsettled sludge in the gravity selector overflow was sent to a clarifier designed with a typical SOR of 1.5 m/h. A stirrer operated at 1 rpm was installed inside the clarifier to prevent sludge from accumulating on the clarifier inner wall. A portion of the sludge settled under this low SOR was wasted daily as WAS for SRT control (Figure 1A). The remainder of the settled sludge was returned to the equalization tank of the PFR as returned activated sludge (RAS) by a peristaltic pump as shown in Figure 1. For the sludge return, the total return flow rate is a sum of the gravity selector underflow rate and the clarifier RAS flow rate. The flow rate ratio between the total return flow and PE was adjusted 3 times during this study. Stable denitrification was finally achieved at a 2:1 ratio of total return flow rate-to-PE flow rate.



(A)



(B)

Figure 1 (A) Schematic diagram and (B) photos of a 10-chamber PFR equipped with a gravity selector, a clarifier, and NRCY flow.

After 180 days of baseline study, 3.3 g/L dry kenaf particles was dosed into the 1st chamber (Figure 1). The kenaf was provided by Nuvoda™ with the specifications shown in Table 1. Due to the clogging problems caused by the dry kenaf hydrophobicity, floating of the kenaf particles occurred and caused several overflow incidents. The clogging problems were mitigated by soaking the dry kenaf for longer time and increasing the gravity selector underflow rate to keep the kenaf moving.

By the end of the project, it was estimated that approximately 2.5 g/L of kenaf remained in the system.

Table 1 Kenaf media specification

Parameter	Value (unit)
Outer surface area	0.076 (m ² /g)
Total surface area (including pores)	1.76 (m ² /g)
Dry density	263 (kg/m ³)
Outer specific surface area	20,000 m ² /m ³ (kenaf media)
Total specific surface area	46300 m ² /m ³ (kenaf media)
Addition in reactor	3.29 (kg/m ³ tank)
Specific gravity	1.056

2.2 Analytical methods

DO was measured using an HQ40D meter (Hach, Loveland, CO, USA). The sludge characteristics such as SVI, zone settling velocity, mixed liquor suspended solid (MLSS) and mix liquor volatile suspended solid (MLVSS) were all analyzed using standard methods (Rice et al., 2012). The samples for sludge characteristics analyses were grabbed from the last chamber of the PFR (Figure 1). The clarifier effluent soluble COD (sCOD), NH₄⁺-N, and NO₃⁻-N concentrations were analyzed using TNTplus® 821, TNTplus® 832, and TNTplus® 835 vials in a Hach DR 5000 UV-Vis Spectrophotometer (Hach, Loveland, CO, USA). The NH₄⁺-N, NO₃⁻-N, and sCOD samples were measured with the filtrate from 0.45 µm syringe filters (EZFlow®, Old Saybrook, CT, USA). The Glucose-glutamic acid solution was used as an artificial substrate to provide sufficient carbon and nutrients for carbonaceous oxygen utilization rate (OUR_{COD}) determination as described in a previous study (An et al., 2023b). For the nitrification oxygen utilization rate (OUR_N) determination, this study used organic carbon free synthetic wastewater with a recipe described in another study (Poot et al., 2016).

2.3 Particle size and image analysis methods.

The particle size distribution was analyzed with two methods. A particle size analyzer (Horiba, LA-950, Kyoto, Japan) was used to directly measure the particle size distribution based on the laser scattering mechanism. As an alternative, the image processing software (ImageJ 2.0.0) was used to indirectly analyze the particle size distribution based on the sample image. To this end, petri dish photos of mixed liquor samples were taken and processed in ImageJ to determine the mean particle size or the surface area of kenaf projected in the petri dish according to method reported elsewhere (Sun et al., 2021).

2.4 Kenaf settling velocity

10 pieces of kenaf were randomly grabbed from the PFR. Each piece of kenaf was dropped in a graduated cylinder to measure its settling velocity by recording the time it took to fall a given distance. The morphology of these kenaf is shown in Figure 2A. The particle sizes of the ten kenaf particles were measured by image analysis and turned out to range from 650 to 1032 μm . Their corresponding settling velocities were determined to be 31.9 ~ 79.1 m/h. Each kenaf particle's size and corresponding settling velocity were plotted in Figure 2B. As can be seen, the settling velocities of the kenaf particles were almost in positively correlated to their particle sizes, i.e., the larger kenaf particles settled faster.

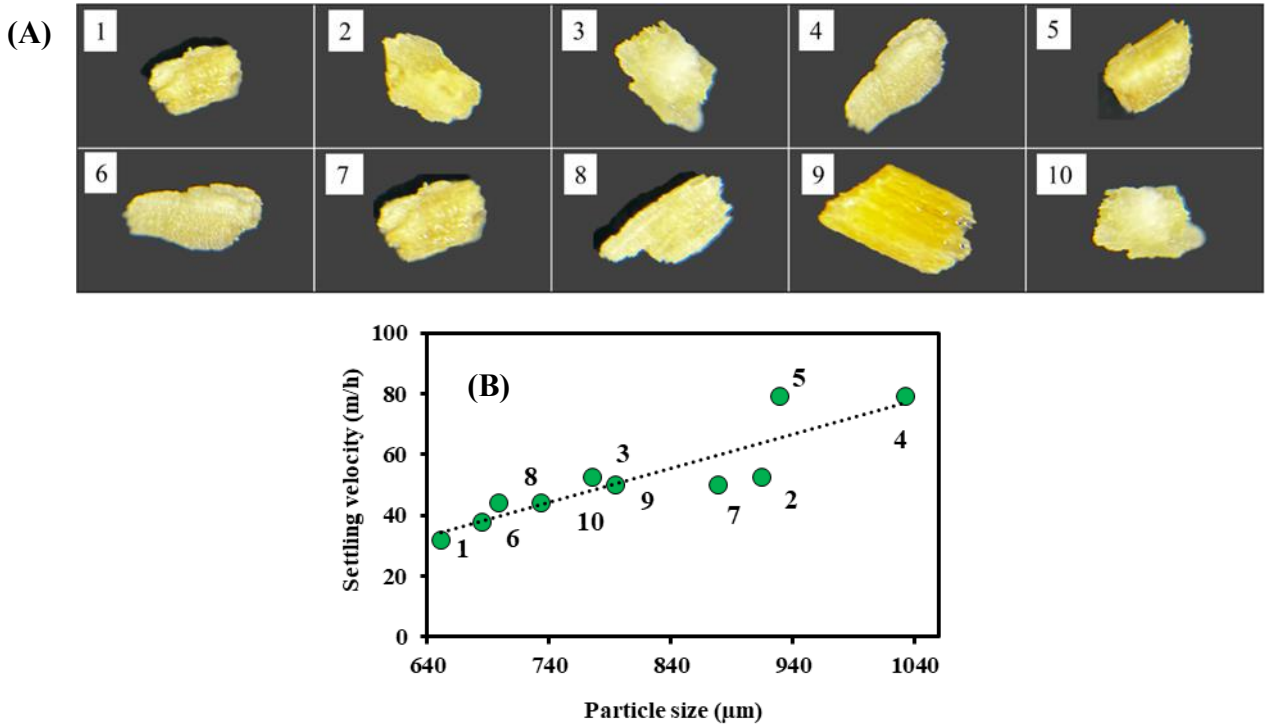


Figure 2 (A) Morphology of 10 pieces of kenaf particles randomly sampled from the pilot reactor, (B) Settling velocity v.s. particle size of the ten randomly collected kenaf particles.

2.5 *Kenaf concentration calibration*

Because kenaf is mingled with the activated sludge, it is quite labor intensive to estimate the kenaf concentration in mixed liquor. We investigated using an image analysis method to indirectly estimate kenaf concentration in the mixed liquor via correlation between the actual kenaf concentration in the mixed liquor and the kenaf concentration estimated from the petri dish image analysis. The goal was to determine whether a calibration can be established between the two to use the results from the quick image analysis to predict the actual mixed liquor kenaf concentration.

For this test we used 250 mL samples collected from various locations of PFR, which were processed through a 500-mesh sieve (Figure 3A) with opening around 27 μm . Deionized water was applied on the sieve to remove sludge and other debris and to leave only kenaf remaining on the sieve (Figure 3B). After processing, the kenaf body was rinsed well enough to expose their original light color (Figure 3C). The rinsed kenaf was transferred to an aluminum dish (Figure 3D) and placed in a 104 ° C oven for 2 hours for the measurement of the kenaf dry weight. This dried sample was then normalized to the original sample volume for calculating the mixed liquor kenaf concentration. 10 mL mixed liquor samples were taken at the same sampling time and locations in the PFR and transferred to a petri dish for image analysis using ImageJ 2.0 software (Figure 3E). Referring to Figures 3F, G, and H, the outline of each kenaf particle can be captured by the software and in turn analyzed for the surface area projection and mean particle size with the length calibrated using a ruler in the same image. Following this, the kenaf surface area per volume of samples was plotted in Figure 3I against the actual kenaf dry mass concentration determined from Figure 3D, i.e., Figure 3I shows the correlation between the kenaf dry mass concentration and the kenaf surface area projection in the unit volume of the mixed liquor measured from the petri dish photos. An $R^2 = 0.99$ indicates that the two parameters are linear correlated, which gave confidence that the image analysis method could be used to predict the actual dry mass concentration of the kenaf in mixed liquor.

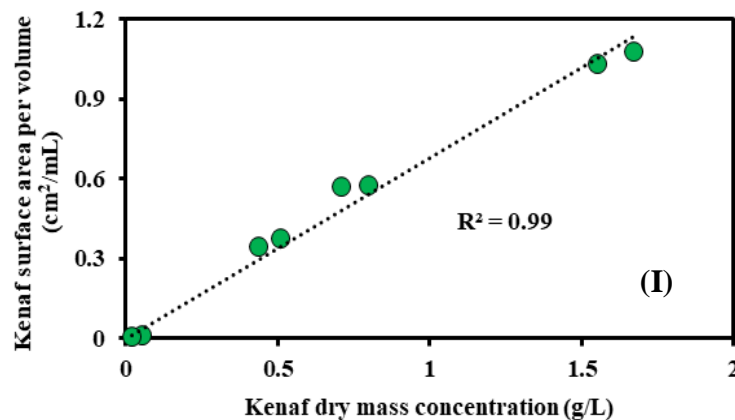
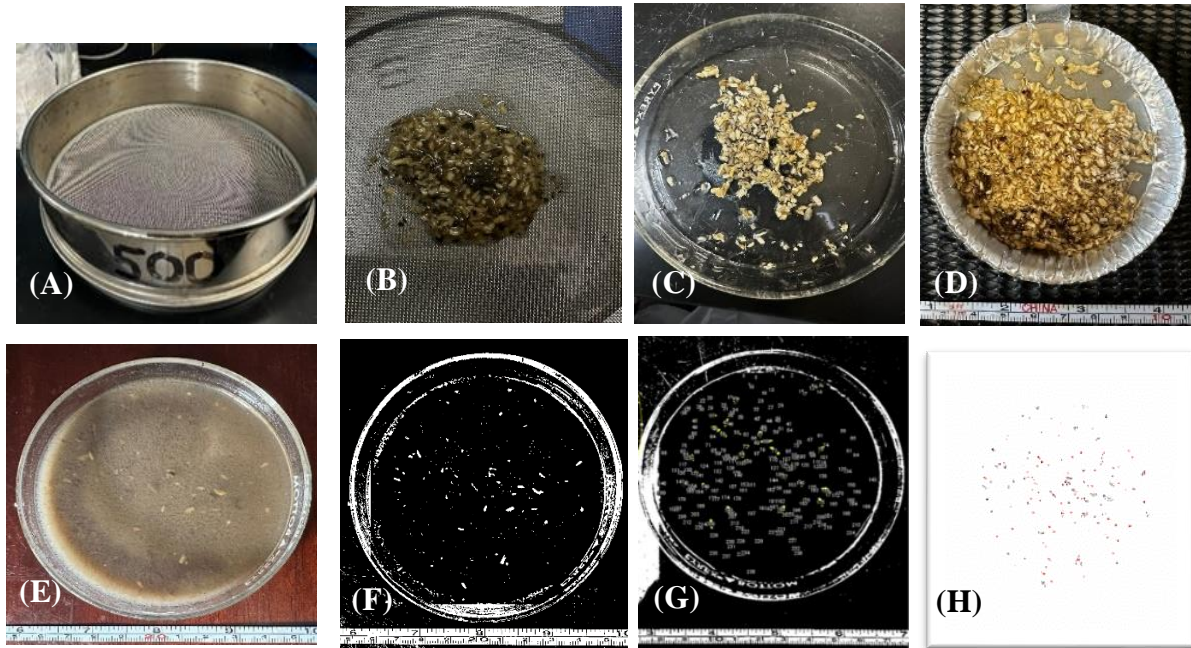


Figure 3 (A) 500-mesh sieve; (B) Kenaf particle separated from 250 mL mixed liquor using sieve; (C) rinsed kenaf body transferred to a petri dish; (D) Kenaf sample transferred into an aluminum dish for dry mass measurement in an oven; (E) Image of a 10 mL mixed liquor sample in a petri dish; (F) Petri dish image processed with bandpass filter using ImageJ 2.0; (G) Identified kenaf particle in the petri dish by ImageJ 2.0; (H) Outline image of kenaf particle available in the petri dish sample, and (I) Correlation between kenaf dry mass concentration and surface area projection in petri dish normalized to the sample volume.

2.6 Confocal microscopy visualization of kenaf surface

The Fluorescence In Situ Hybridization (FISH) method was employed to enable confocal microscopy visualization of microbial distribution on kenaf surface by using EUB338 probe with sequence (5'–3'): [TxRd] GCTGCCTCCCGTAGGAGT (Sigma-Aldrich) which targets almost all bacterial DNA. The method consists of five steps, i.e., slide cleaning and coating, sample fixation, sample dehydration, sample hybridization, and confocal microscopy visualization. To clean and coat slides, slides were dehydrated in 100% ethanol twice for 5 min each, treated with RNase solution (0.1 mg/mL) for 30-60 mins at 37° C, and then coated with poly-L-lysine before drying. To fix kenaf samples, the samples were mixed with 4% paraformaldehyde in a sample-to-paraformaldehyde volumetric ratio of 1:3 and then stored at 4°C for overnight. To dehydrate the kenaf samples, the fixed samples were centrifuged to remove paraformaldehyde and replenished with the equivalent volume of phosphate buffered saline (PBS). Then, the samples were centrifuged again to remove PBS. During dehydration, the fixed sample was applied to the clean and coated slides, dried at 46°C, and submerged in ethanol solutions of increasing concentration (50%, 80%, 96%) to remove residual moisture for 3 min each. For hybridization, each sample was covered with 10 µL hybridization buffer and 1 µL of the EUB338 probe labeled with Texas Red dye. The slide was placed in a humidified chamber and incubated at 46°C for 90 min. After hybridization, unbound probes were removed in a pre-heated (48°C) washing buffer, and then the slide was rinsed with nucleus-free water and air-dried. In the final step, an anti-fading reagent was applied, and the sample was covered with a cover glass. The microscopic glass slides containing kenaf slices were observed using a Zeiss LSM 880 confocal laser scanning microscope.

A near-UV laser with a wavelength of 405 nm was used to capture auto-fluorescent images of the kenaf surface, while a HeNe2 laser with a wavelength of 594 nm was used to detect bacterial cells scattered on the kenaf surface.

CHAPTER 3: RESULTS

3.1 Sludge settleability before and after kenaf addition

The primary goal of this study was to investigate the mechanism for improved sludge settling when adding plant-based material such as kenaf as a ballasting migrating carrier. Both SVI and zone settling velocity have been used as the indicators of sludge settleability. A baseline study was conducted between 7/3/2023 and 10/31/2023 for 120 days to measure the ranges of SVI and zone settling velocity without kenaf addition. As shown in Figure 4A and B, the baseline SVI and zone settling velocity values fluctuated in the ranges of 150 ~ 200 mL/g and 1~ 4 m/h, respectively. Because the optimum SVI and zone settling velocity of activated sludge should be in the ranges of 50 ~ 150 mL/g and greater than 2 m/h (Metcalf, 2003), these baseline data evidenced the poor settleability of the sludge and emphasized the importance of this study. On day 120, 3.3 g/L kenaf was dosed into chamber 1 in Figure 1. As can be seen from Figure 4A, the SVI dramatically dropped from 170 ± 20 to 60 ± 10 mL/g over the 106 days after kenaf addition, indicating the essential role that kenaf has played. Because SVI was calculated by the settled sludge volume ratio (mL/L) to MLSS, one may argue that SVI improvement could be the result of the increased MLSS due to kenaf addition and thus unnecessarily mean real sludge settleability improvement. To investigate this possibility, the settled sludge volume ratio (mL/L), namely the numerator of the SVI, with and without kenaf addition was plotted against MLSS in Figure 4C. Before the addition of kenaf, at an MLSS concentration of 2500 mg/L (on 9/26/23), the settled sludge volume was

measured at 430 ml. In contrast, after kenaf was added, at a higher MLSS concentration of 4000 mg/L with concentration of 2800 mg/L of sludge and 1200 mg/L of kenaf (on 2/8/24), the settled sludge volume decreased to 340 ml. This comparison clearly shows that, even with a higher sludge concentration after kenaf addition, the settled volume was lower than before kenaf addition. Theoretically, a higher sludge concentration should result in a greater settled volume. However, the reduction in settled volume after kenaf addition demonstrates that kenaf promotes better sludge compression, leading to denser sludge flocs. A photo taken during the SVI test in Figure 4D revealed that the white kenaf fibers were evenly mingled with the sludge and did not settle down to the bottom of the sludge blanket, even though their settling velocities were 10 times faster than the sludge blanket (Figure 2B). The uniform distribution of kenaf in settled sludge blanket suggested that the kenaf particles must have flocculated with the sludge flocs in the early stage of the settling and went through the hindered and compressed settling together. This entrapment of kenaf in settled sludge blanket resembles the results of ballasted flocculation that have been studied previously (Ghanem et al., 2007). The heavier kenaf (Table 1) in the sludge matrix must have compressed the volume of the settled sludge matrix as shown in Figure 4D. This inference corroborated with the zone settling velocity data in Figure 4B, i.e., after kenaf addition, the zone settling velocity of the sludge blanket dramatically increased from 2.5 ± 0.5 m/h to 6.5 ± 0.5 m/h over the 106 days after kenaf addition. The three times greater zone settling velocity because of kenaf addition indicated the essential role that kenaf has played in dragging down the entire sludge blanket after being incorporated into the sludge matrix (Figure 4D).

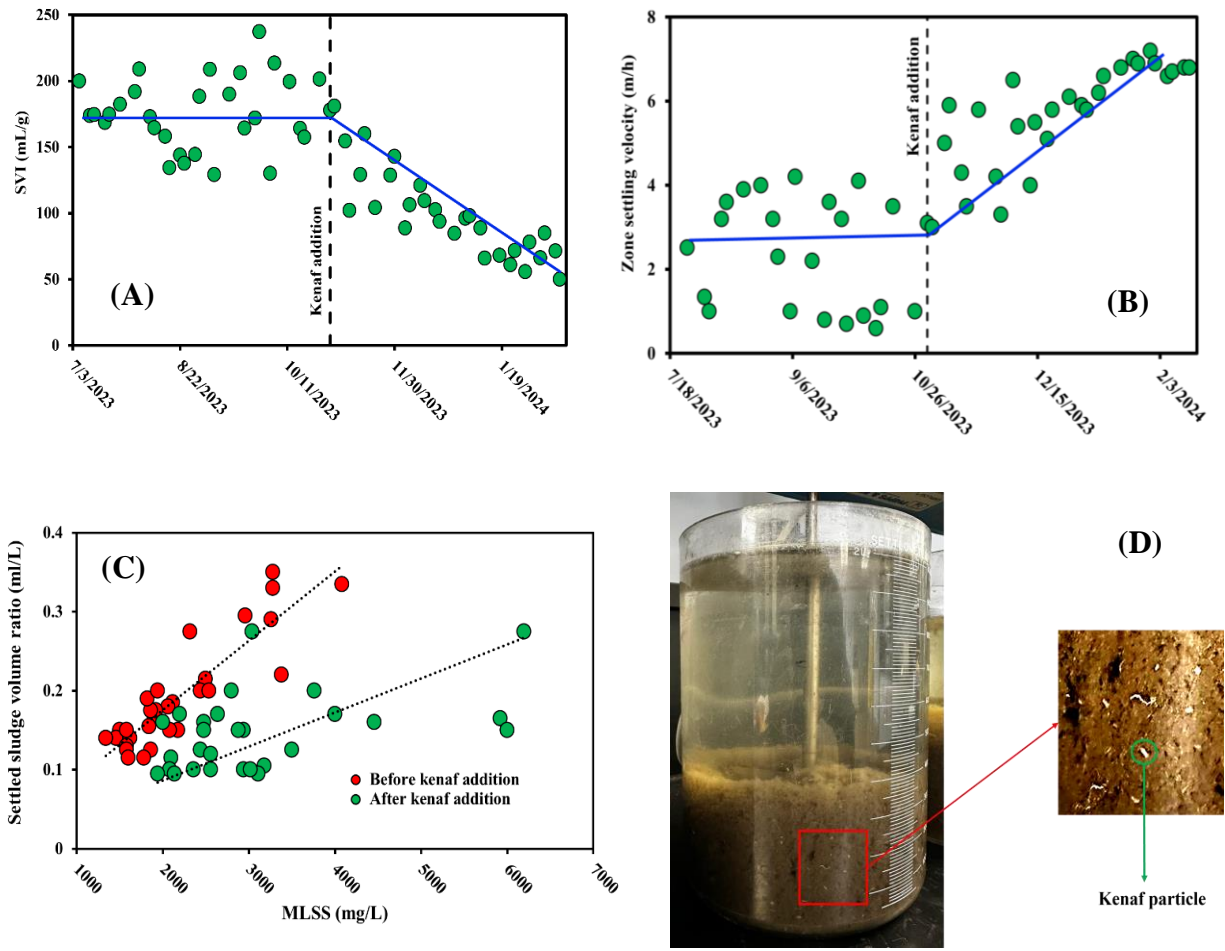


Figure 4 Profiles of (A) SVI and (B) zone setline velocity before and after kenaf addition; (C) Settled sludge volume ratios measured at various MLSS; (D) An image of kenaf particles (white) mingled within the sludge blanket observed during SVI test after 30 min settling.

3.2 Treatment performance before and after kenaf addition

In terms of the treatment performance, the baseline data collected between 5/4/2023 and 2/14/2024 revealed that the influent sCOD removal efficiency was around $70 \pm 10\%$ with effluent sCOD level stabilizing around 10 ± 3 mg/L (Figure 5A). Because the level of this residual sCOD was in the

same range as that in the full-scale secondary effluent in the same WRRF (data not shown), we can regard this residual sCOD as non-readily biodegradable. As for $\text{NH}_4^+\text{-N}$, almost 100% removal was achieved during the baseline study with effluent controlled to be below 1 mg/L (Figure 5B), meeting the permissible effluent concentration of this WRRF. Although there was negligible influent $\text{NO}_3^-\text{-N}$ concentration, the effluent $\text{NO}_3^-\text{-N}$ concentration was controlled to be around 12 ± 4 mg/L during the baseline study through MLE-enabled denitrification in the PFR by using the influent COD as the electron donor without any external carbon addition (Figure 5C). This full scale-mimicking MLE setup in the pilot PFR successfully removed $62\pm 5\%$ influent TIN and brought down the effluent TIN to 7 ± 3 mg/L which was below the permissible discharge level.

Upon kenaf addition on 10/31/2023 (Figure 5), all treatment performance quickly deteriorated during the first seven days because of the clogging issue encountered in the PFR. Briefly, the clogging of the kenaf in the pipeline led to the loss of sludge inventory through the treatment tank overflow. After fixing the clogging issues, all treatment performance indicators, i.e., effluent concentrations of sCOD, $\text{NH}_4^+\text{-N}$, $\text{NO}_3^-\text{-N}$, and TIN as well as their removal efficiencies returned to the levels of baseline or even better (Figure 5).

The addition of kenaf significantly enhanced the return of active biomass concentration within the system through the gravity selector underflow and return activated sludge (RAS) from the secondary clarifier, compared to baseline conditions before kenaf addition. Prior to kenaf addition, the average Volatile Suspended Solids (VSS) concentration from the combined underflow and RAS was 9480 mg/L. After the introduction of kenaf, this value increased to 12,620 mg/L, indicating a substantial improvement in biomass inventory within the system (Figure 5E and F).

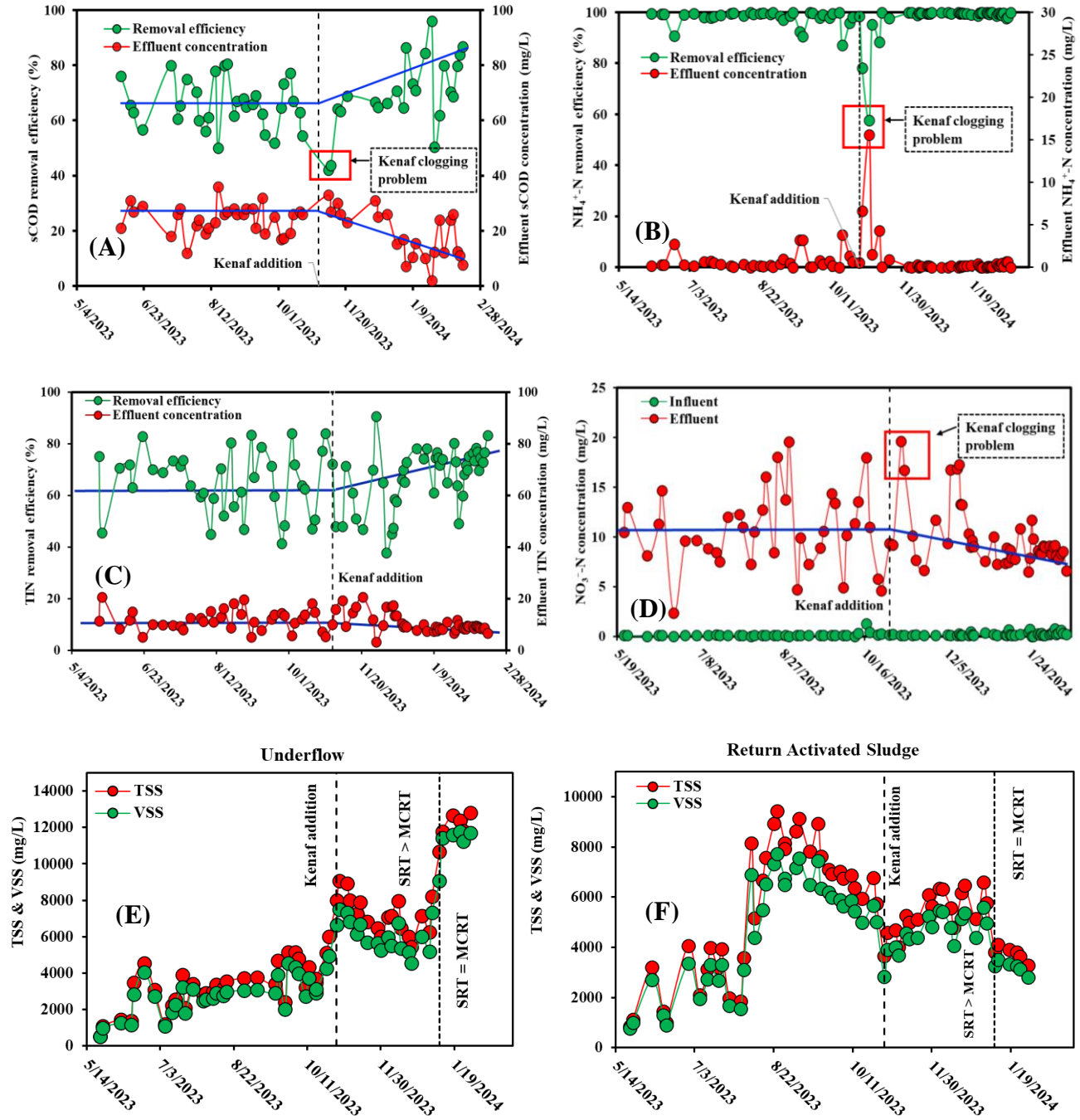


Figure 5 Removal efficiencies and effluent concentrations of (A) sCOD, (B) $\text{NH}_4^+\text{-N}$, and (C) TIN before and after kenaf addition, (D) $\text{NO}_3^-\text{-N}$ influent and effluent concentration profiles before and after kenaf addition, (E) TSS & VSS concentration of gravity selector underflow, and (F) TSS & VSS concentration of return activated sludge.

This higher return of active biomass contributes directly to improved treatment performance, particularly by enhancing soluble Chemical Oxygen Demand (sCOD) removal efficiency. Thereby, the comparable or even better treatment performance before and after kenaf addition suggested that there was no treatment performance compromise even though the inactive kenaf has occupied a fraction of the sludge inventory.

3.3 Effectiveness of the gravity selector in retaining and returning kenaf

The gravity selectors used in this study had been previously used for providing gravity selection pressure to drive aerobic granulation (An et al., 2023; Sun et al., 2021). In theory, all particles that can settle faster than the upflow velocity set for the gravity selector will be retained in the selector bottom and then returned as underflow to the front of the PFR as shown in Figure 1. The remaining particles will be washed out via selector overflow into the clarifier, where some will be returned to the front of the PFR, and the rest will be wasted as WAS (Figure 1). The effectiveness of this gravity selector in selectively retaining kenaf was investigated during this study.

The underflow rate of gravity selector had to be increased twice from 22% to 24% and then to 29% of total flow rate which was two times the PE flow rate. The purpose of this underflow rate increase was to keep the settled kenaf moving from the bottom of gravity selector to mitigate the clogging issues encountered right after kenaf addition. By sieving and rinsing methods demonstrated in Figure 3A to D, the dry mass of kenaf and activated sludge in mixed liquor can be separately measured. Referring to Figure 6A, around $69\pm 2 \sim 79\pm 3\%$ of influent kenaf and $60\pm 5 \sim 75\pm 5\%$ influent sludge was partitioned into the gravity selector underflow at the three ratios of underflow-

to-total return flow rate used in this study. These solid partition values were substantially greater than the flow rate partition values (Figure 6A), indicating the effectiveness of the gravity selector in retaining and returning solids.

Figure 6B shows the particle size distribution. After adding kenaf, both the underflow and overflow particles exhibited size increase, and the increase became even more substantial in December 2023 after the kenaf clogging issues were resolved. The substantially greater particle size increase in the underflow over that in the overflow further suggested that the gravity selector was selectively retaining large solid particles such as kenaf and flocculated sludge matrix.

Although Figure 6A has demonstrated that majority of the sludge partition into the underflow, it is necessary to confirm whether these sludges were active or not because inert particles also could be heavier and partitioned into the gravity selector underflow. To address this unknown, both OUR_{COD} and OUR_N were measured in the inflow and underflow, and their partition in the underflow were plotted in Figure 6C to reflect the fractions of active heterotrophs and nitrifiers partitioned in the underflow. Results in Figure 6C suggested that almost equal fractions of heterotrophs and nitrifiers in the range of $74\pm 2\%$ ~ $77\pm 2\%$ consistently partitioned into the underflow during 1/18/2024 – 2/6/2024, which was almost the same as the fractions of sludge partitioned into the underflow during the same period as shown in Figure 6A. These results are very different from those reported for aerobic granular sludge formed in the same PFR in a previous study (An et al., 2023a). When the same gravity selector was applied to drive continuous flow aerobic granulation, the underflow was found to selectively favor the retention of nitrifiers over heterotrophs for their different SRTs in the PFR (An et al., 2023a). The non-differential retention of nitrifiers and

heterotrophs observed in Figure 6C just revealed that the sludge densification mechanisms behind ballasted flocculation and aerobic granulation are essentially different.

Because of the heavier nature of kenaf (Table 1), its content in gravity selector underflow was reasonably greater than that in the overflow. As a consequence, the activated sludge contents in the overflow became higher than in the influent mixed liquor regardless of the underflow rate (Figure 6D). Since the overflow and WAS should share the same activated sludge content in the suspended solids, this higher activated sludge contents in the WAS than in the mixed liquor may impact the sludge SRT which is discussed in the next section. It should be also realized that the kenaf ended up in the overflow, even though minor amount, has the risk to be lost from the PFR through WAS removal.

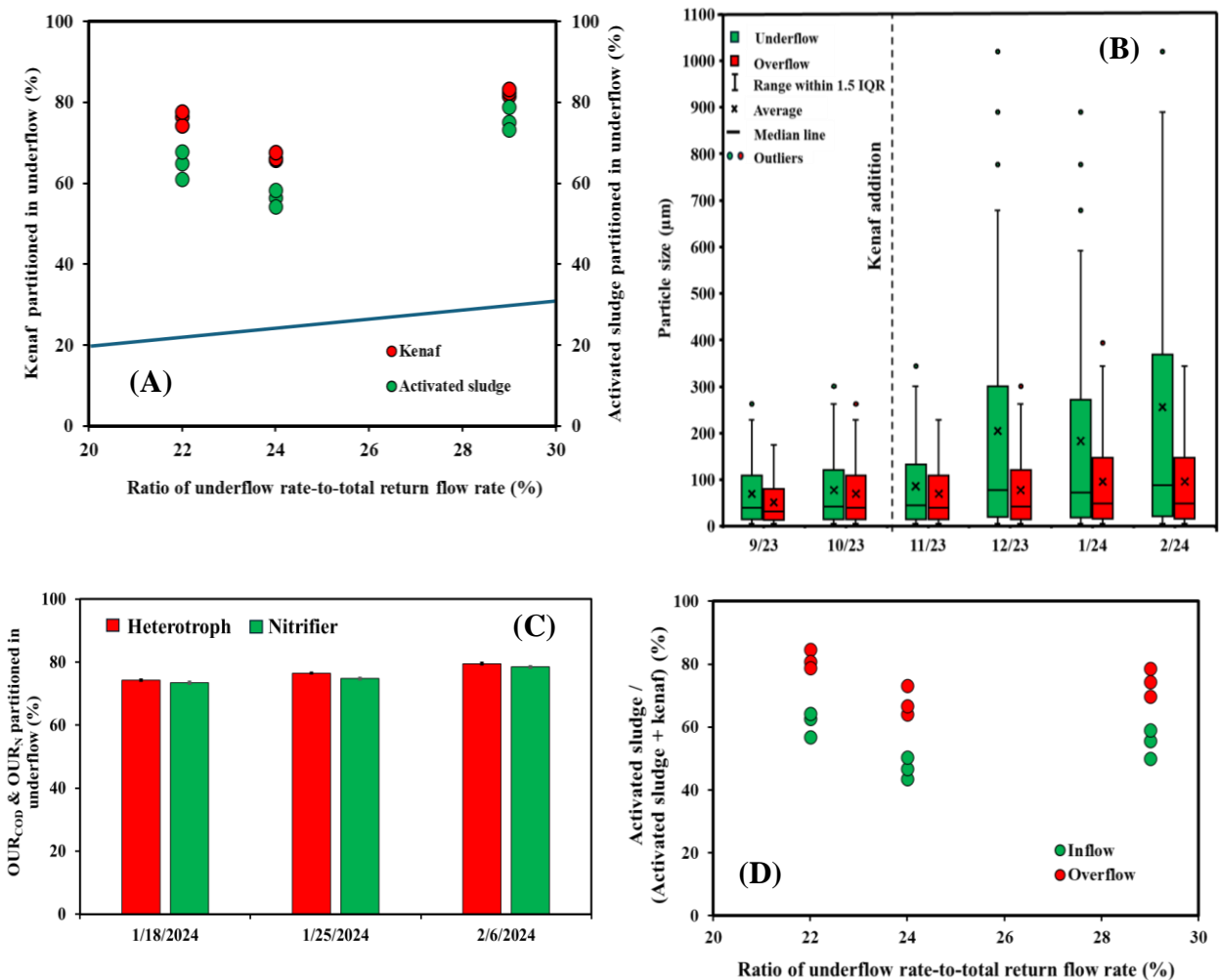


Figure 6 (A) Fractions of kenaf and activated sludge partitioned into the underflow at different ratios of underflow rate-to-total return flow rate which is also indicated by the blue line; (B) Particle size distribution profile determined by particle size analyzer for underflow and overflow grabbed samples before and after kenaf addition. The box-whisker plot was used in which average particle size was indicated by × symbol with upper and lower whisker boundary of 1.5 Interquartile range (IQR); (C) Fractions of heterotrophs and nitrifiers partitioned into the underflow; and (D) The biomass contents of activated sludge in gravity selector inflow and overflow.

3.4 Development of a novel SRT control method specifically tailored for using kenaf as a ballasting agent

The baseline sludge inventory in terms of MLSS and MLVSS in Chamber 10 stabilized around 3300 ± 200 mg/L and 2700 ± 300 mg/L during 30 days prior to the kenaf addition (Figure 7A). After kenaf addition, it can be seen from Figure 7A that both MLSS and MLVSS kept decreasing even beyond the seven days of clogging troubleshooting. Analyzing the reason behind, one hypothesis was that the inactive kenaf biomass might have misled the SRT calculation and led to a shorter than designed SRT in the PFR. Traditionally, SRT is a key parameter used by operators to control the sludge inventory. SRT represents the retention time of all suspended solids in a bioreactor and was calculated by the reactor total suspended mass divided by mass of suspended solid in WAS removed on a daily basis. With kenaf mingled within the activated sludge as shown in Figure 4D, the SRT calculation becomes,

$$SRT = \frac{(X_S + X_K) \times V}{Q_{WAS} \times (X_{S_WAS} + X_{K_WAS})} \quad (1)$$

in which X_S and X_K stand for the concentrations of activated sludge and kenaf in the mixed liquor, respectively; X_{S_WAS} and X_{K_WAS} stand for the concentrations of activated sludge and kenaf in the WAS, respectively; V stands for the PFR volume, and Q_{WAS} stands for the WAS flow rate. Eq. 1 revealed that SRT regulates the retention of both inactive kenaf and activated sludge as a whole without differentiation. This non-differential solids retention might have misled the true purpose of the SRT control, namely regulate the mean cell residence time (MCRT) which does not include the inactive kenaf. MCRT can be calculated in Eq. 2,

$$MCRT = \frac{X_S \times V}{Q_{WAS} \times X_{S_WAS}} \quad (2)$$

Dividing Eq. 2 by Eq. 1 gives,

$$\frac{MCRT}{SRT} = \frac{\frac{X_S}{(X_S + X_K)}}{\frac{X_{S_WAS}}{(X_{S_WAS} + X_{K_WAS})}} \quad (3)$$

According to Figure 6D, the activated sludge content in the gravity selector overflow was much greater than that in the influent mixed liquor because of the selective retention of kenaf in the underflow, which means,

$$\frac{X_S}{(X_S + X_K)} < \frac{X_{S_WAS}}{(X_{S_WAS} + X_{K_WAS})} \quad (4)$$

Substituting Eq. 4 into Eq. 3 derives,

$$MCRT < SRT \quad (5)$$

Therefore, Eq. 5 explains the loss of sludge inventory observed in Figure 7A, i.e., because of the interference of inactive kenaf, the MCRT was uncoupled from SRT and turned out to be lower than the SRT, which led to more activated sludge discharged with WAS than when MCRT = SRT. Because kenaf is also part of the MLVSS measured in the standard method, there is no way to exclude kenaf from SRT calculation in Eq. 1 if the standard methods are used. That being said, a novel method capable of quickly differentiating MCRT from SRT in this kenaf mingled system is required. Although the sieving and rinsing method used in Figure 3A to D was able to differentiate kenaf from sludge, we believe that method is too complicated for WRRF operators to adopt. Instead, we explored an OUR-based approach to exclude kenaf from SRT calculation so as to make SRT = MCRT because the inactive kenaf does not count towards OUR readings. Thereby, Eq. 1 can be re-written as Eq. 6 regardless of the kenaf interference,

$$SRT = MCRT = \frac{OUR_N \times V}{Q_{WAS} \times OUR_{N_WAS}} \quad (6)$$

in which OUR_N and OUR_{N_WAS} represent the nitrification oxygen utilization rate measured in the mixed liquor and WAS, respectively. Figure 7B demonstrates the difference in WAS flow rate

regulated by Eqs. 1 and 6, respectively. Consistent with the prediction in Eq. 5, the traditional SRT control using Eq. 1 always overestimates the WAS discharge as compared to the OUR-based SRT control in Eq. 6 (Figure 7B). Hence, starting from 1/11/2024, Eq. 6 was used to calculate SRT. Figure 7A revealed that the MLVSS dramatically increase from 2000 ± 380 to 4100 ± 320 mg/L following the switch to OUR_N -based SRT control (Eq. 6), verifying the effectiveness of this new SRT control strategy in the context of kenaf being used as a ballasting agent.

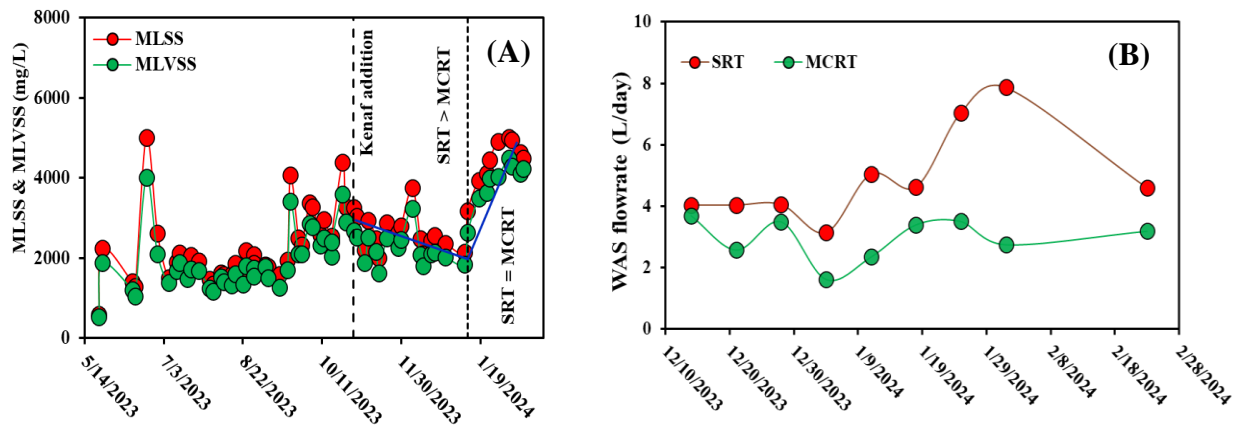


Figure 7 (A) MLSS and MLVSS concentrations measured in Chamber 10; (B) WAS flowrate calculated based on SRT using MLSS in Eq. 1 and MCRT using OUR in Eq. 6, respectively.

3.5 Monitoring of kenaf settling in sludge blanket

To understand how kenaf helped improve sludge settleability, a column settling test was performed to monitor the settling dynamics of kenaf particles along the height of a 100 cm column at a 10 min interval over 30 min. The image analysis method illustrated in Figure 3E to I was employed to quantify the kenaf particles by their surface area and mean size. The dynamic images and profiles Figure 8 showed that at 0 min, kenaf mingled in the sludge was evenly distributed throughout the column heights from top to bottom. After 10 mins, there was no kenaf at the top of

the column but the quantity of kenaf observed at the bottom of the column was greater than those observed at all other height of the column. This trend was kept over the test duration. After 30 min, although many kenaf particles settled at the bottom of the column, there are still considerable kenaf particles being suspended at the column height of 20 cm and 40 cm as detected by the surface area and size of the kenaf measured in Figure 8C and D. It should be realized that the surface area detected by the imaging analysis is directly proportional to the kenaf dry mass (Figure 3I). The discrete settling velocities of kenaf particles were measured to be in the range of 32 to 70 m/h (Figure 2B), according to which all kenaf particles should have settled to the bottom of the column within 2 min. The fact that large amount of kenaf still remained suspended at 20 cm and 40 cm column height after 30 min just revealed that kenaf particles must have been trapped within the flocculated sludge matrix in the early stage of the settling and gone through the hindered and compressed settling together. This entrapment of kenaf in settled sludge blanket resembles the results of ballasted flocculation that have been studied previously (Ghanem et al., 2007).

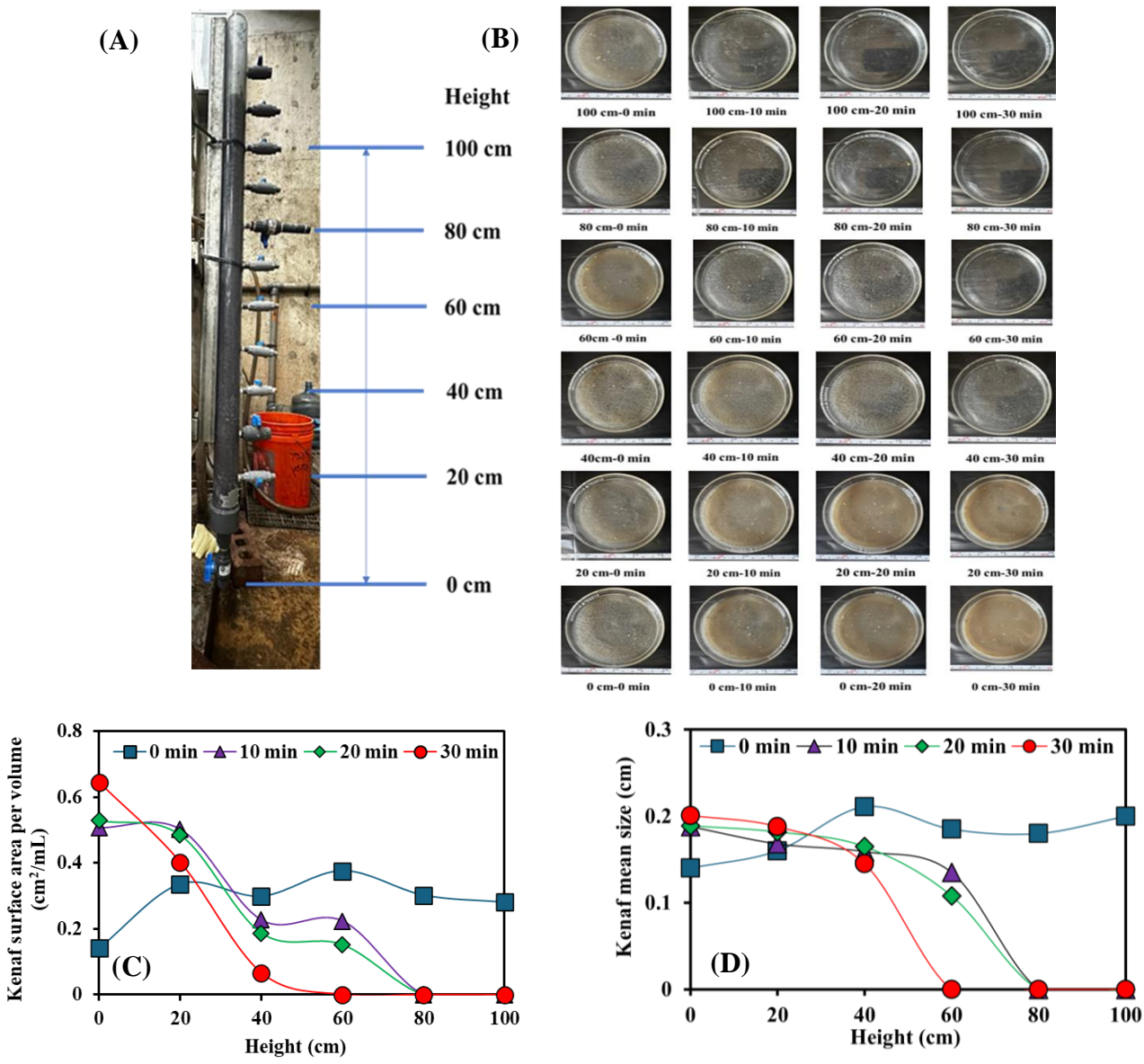


Figure 8 (A) The setup of a column settling test that allows samples to be taken at various heights of a column; (B) Petri dish images of samples taken from different column heights at various sampling time, (C) Kenaf surface area present in unit volume of samples, and (D) Kenaf mean sizes measured at the different settling time and height of the column.

3.6 Confocal microscopy visualization of the kenaf surface

After FISH treatment of the kenaf particles with EUB338 probe targeting eubacteria, a comparison of the confocal channel with auto-fluorescence only (Figure 9A) and with laser beam at a wavelength of 594 nm (Figure 9B) is shown in Figure 9. It was not difficult to observe that there was no biofilm formed on the kenaf surface even after 105 days of kenaf addition in the PFR. Instead, only a few bacterial cells randomly scattered on the kenaf surface in Figure 9B.

The formation of a biofilm starts when free-floating microorganisms attach to the surface. For this process to occur, microorganisms typically prefer hydrophobic surfaces because hydrophobic interactions make it easier for them to anchor and form colonies. In contrast, hydrophilic surfaces like kenaf are less favorable for biofilm formation because they do not support strong microbial attachment. The initial attachment of microorganisms to a surface is mediated by weak forces such as van der Waals interactions and hydrophobic effects (Briandet et al., 2001). Once attached, microorganisms may secure themselves more permanently using cell adhesion structures. However, the hydrophilic nature of the kenaf surface makes it unfavorable for such attachment. Therefore, the hydrophilic property of kenaf prevents microorganisms from attaching and forming biofilms, even after long cultivation. This explains why no biofilm was observed on the kenaf surface in this study. The surface's hydrophilicity creates an environment that is naturally resistant to microbial colonization and biofilm development. So, it just reconfirmed the role that kenaf played for sludge densification was through ballasted flocculation but not as the biofilm carriers.

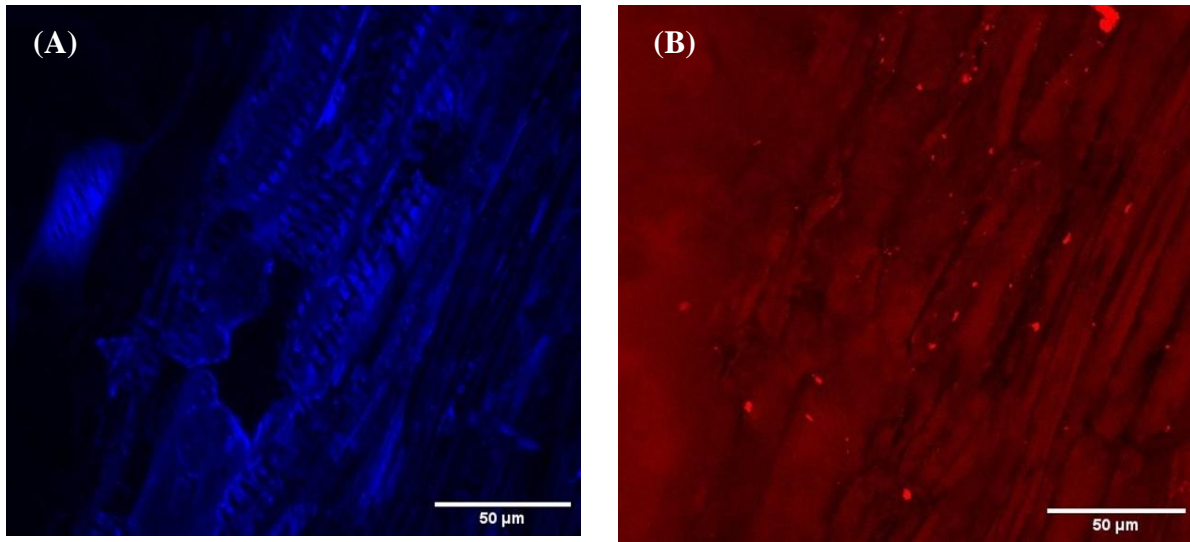


Figure 9 Confocal microscopy visualization of the (A) auto-fluorescent image of kenaf surface, and (B) bacterial cells scattered on kenaf surface. Sample was taken 105 days after kenaf addition.

CHAPTER 4: DISCUSSION

4.1 Mechanism of kenaf-enhanced sludge settleability

Figure 4A to C evidenced the essential role that kenaf has played in improving the sludge settleability in terms of SVI and zone settling velocity. Figures 4C and D even suggested that this role was possibly played through the ballasting of the sludge blanket by the kenaf particles that have been incorporated into the sludge matrix, which explains the kenaf distribution profiles over time measured in the column settling tests in Figure 8, i.e., a substantial amount of kenaf remained suspended in the sludge blanket even after 30 min settling, which compressed the settled sludge volume as indicated in Figure 8C and D. This ballasting role of kenaf can be further inferred from the microscopic evidence that there was no biofilm formation on kenaf surface even after 105 days of cultivation (Figure 9). This ballasting role of kenaf was even played in the gravity selector where the HRT was only 7 min, which not only allowed majority of the kenaf to be collected from the underflow but also increased the active biomass content in the underflow to the level about three times that in the overflow (Figure 6A and C).

There are two theories explaining the roles of ballasting materials played during expedited settling. One of them was put forward by Chang et al. (1998) and described the ballasting materials functioning as a "seed" for the floc formation through the firm attachment of flocs on the ballasting material surfaces. The other theory put forward by Ghanem et al. (2007) described the role of ballasting materials as the heavy ingredient incorporated through momentum into the matrix of flocculants that have already been formed during settling. Based on the microscopic visualization

in Figure 9, the lack of biofilm formation on kenaf surfaces suggested that the first theory may not apply, and the second theory might provide a better explanation of the mechanism behind kenaf-enhanced sludge settling. It is highly possible that collision between the sludge flocculants and kenaf particles during settling has allowed the kenaf with greater mass to hit and enter the flocculated sludge matrix by momentum which is depicted in Figure 10. During settling, these kenaf-incorporated large sludge matrix might have swept other sludge flocs in the aqueous phase through differential settling velocity and in turn formed even larger ballasted flocs. The much greater density of kenaf must have dragged the entire kenaf-incorporated sludge matrix to settle in an accelerated way as indicated by the zone settling velocity in Figure 4C and the quick separation in the gravity selector (Figure 6).

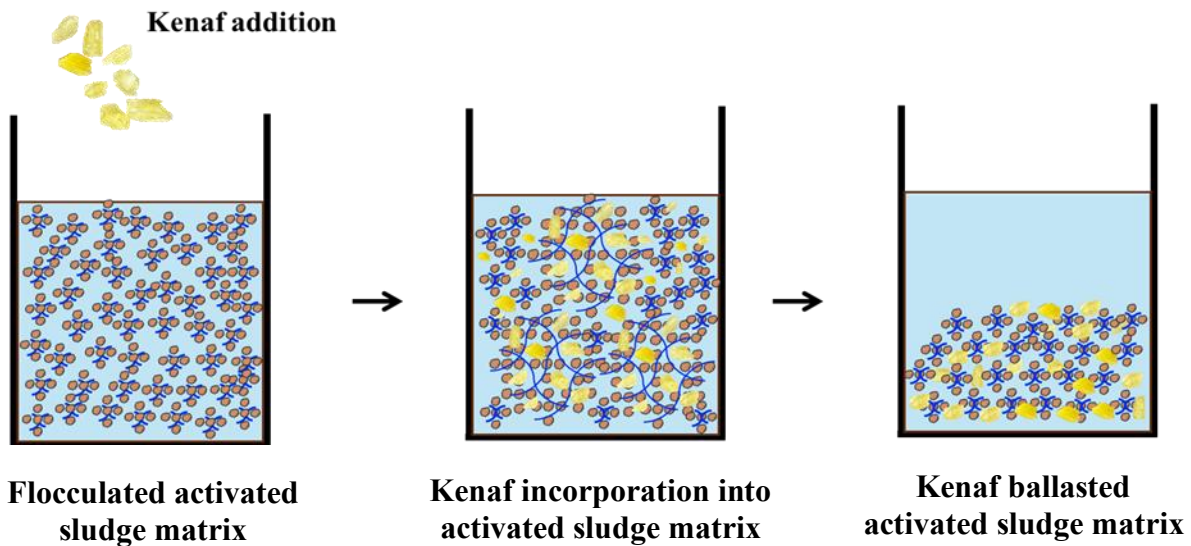


Figure 10 Schematic illustration of the mechanism of kenaf-enhanced sludge settleability.

4.2 Lessons learned from this study

Two lessons were learned from this study and should be avoided in the future application of the technology. The first lesson has to do with the severe clogging issues encountered soon after the ‘dry’ kenaf addition. It was the initial dry kenaf hydrophobicity that caused the product to float on the water surface rather than becoming homogeneously dispersed in the mixed liquor as originally expected (Figure 11A and B). Consequently, the floating kenaf quickly clogged the tubing (Figure 11C) and connectors (Figure 11D), resulting in system overflow and sludge inventory loss. Of course, the small size of the pilot reactor components might have contributed to the clogging issue which may not become a real problem in full-scale systems. However, the floating problem in Figure 11A could be an issue leading to kenaf loss through hydrocyclone overflow and WAS discharge. Countermeasure needs to be in place to avoid the same problem in full-scale application. To that end, soaking kenaf in water overnight before adding it into the treatment train was confirmed to be helpful for mitigating the kenaf floating and clogging problems by swiftly allowing kenaf particles to be homogeneously mixed with the activated sludge. Other than pre-soaking kenaf, increasing the flow rate was also found to be helpful for mitigating clogging. This measure was used to unclog the underflow of the gravity selector.

Another lesson learned was that the traditional SRT control method is not applicable anymore in treatment trains with gravity selector or hydrocyclone installed. The selective retention of the inactive kenaf particles in underflow led to overestimation of the WAS discharge. Therefore, a method that can exclude interference of inactive kenaf from the SRT calculation should be employed. Although the sieving and rinsing methods used in Figure 3A to D allow the

differentiation of the kenaf from activated sludge, the method appeared to be too time-consuming for operators to adopt. Instead, this study has proven that the OUR-based SRT control as shown in Eq. 6 is relatively easier to implement and can accurately achieve the SRT control at the designed levels (Figure 7). In turn, training operators to measure and use OUR for SRT calculations could provide a practical solution.

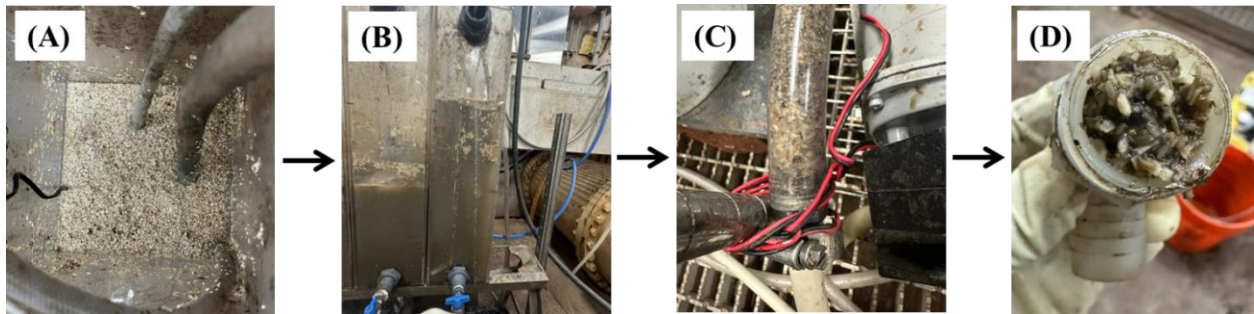


Figure 11 (A) Kenaf floating on the mixed liquor surface; (B) Water level difference caused by tubing clogging between chambers; (C) Tubing being clogged by kenaf; (D) Kenaf clogging tubing connectors.

CHAPTER 5: CONCLUSIONS

The following concluding remarks can be drawn from this study:

1. Kenaf addition rapidly enhanced sludge settleability, showcasing its potential as an effective ballasting agent.
2. There was no treatment performance loss from adding kenaf into the sludge inventory, except for the impact of the accidental clogging issue.
3. Gravity selector can effectively retain majority of the kenaf in the underflow while minimizing their washout through the overflow.
4. The essential role that kenaf played can be presumably attributed to the incorporation of kenaf into the sludge matrix through momentum during flocculation. This is different from the ‘seed’ making mechanism relying on sludge attachment on the kenaf surfaces.
5. Due to the greater sludge content in the WAS than that in the mixed liquor as a result of the selective retention of kenaf in the underflow, the traditional SRT calculation overestimated the WAS discharge and in turn decreased the sludge inventory. An OUR-based SRT calculation method was proven to be effective in correcting the SRT calculation.
6. A seamless transition from a conventional activated sludge system to a kenaf-ballasted activated sludge system can be expected without significant treatment performance interruptions if proactive measures are taken to avoid the dry kenaf floating.

REFERENCES

- An, Z., Wang, J., Zhang, X., Bott, C.B., Angelotti, B., Brooks, M. and Wang, Z.-W. 2023. Coupling physical selection with biological selection for the startup of a pilot-scale, continuous flow, aerobic granular sludge reactor without treatment interruption. *Water Research X* 19, 100186.
- Bauhs, K., Armenta, M., Maltos, R., Sturm, B. and Regmi, P. 2024. Making waves: Riding the densification wave from current understanding to advancement. *Water Research*, 121690.
- Boltz, J.P. and Daigger, G.T. 2022. A mobile-organic biofilm process for wastewater treatment. *Water Environment Research* 94(9), e10792.
- Briandet, R., Herry, J.-M. and Bellon-Fontaine, M.-N. 2001. Determination of the van der Waals, electron donor and electron acceptor surface tension components of static Gram-positive microbial biofilms. *Colloids and Surfaces B: Biointerfaces* 21(4), 299-310.
- Chhuon, R., Shahid, M.K., Kim, S. and Choi, Y. 2020. Mill scale as a ballasted flocculant for enhancing the settleability of activated sludge. *Journal of Environmental Chemical Engineering* 8(5), 104237.
- Ford, A., Rutherford, B., Wett, B. and Bott, C. 2016 *Implementing Hydrocyclones in Mainstream Process for Enhancing Biological Phosphorus Removal and Increasing Settleability through Aerobic Granulation*, Water Environment Federation.
- Franca, R.D., Pinheiro, H.M., van Loosdrecht, M.C. and Lourenço, N.D. 2018. Stability of aerobic granules during long-term bioreactor operation. *Biotechnology Advances* 36(1), 228-246.

- Gasperi, J., Laborie, B. and Rocher, V. 2012. Treatment of combined sewer overflows by ballasted flocculation: Removal study of a large broad spectrum of pollutants. *Chemical Engineering Journal* 211, 293-301.
- Kent, T.R., Bott, C.B. and Wang, Z.-W. 2018. State of the art of aerobic granulation in continuous flow bioreactors. *Biotechnology Advances* 36(4), 1139-1166.
- Kumar, S., Kazmi, A.A., Ghosh, N.C., Kumar, V. and Rajpal, A. 2019. Urban stormwater runoff treatment of Nainital Lake's catchment: an application of ballasted sand flocculation technology. *Water Supply* 19(4), 1017-1025.
- Lee, D.-J., Chen, Y.-Y., Show, K.-Y., Whiteley, C.G. and Tay, J.-H. 2010. Advances in aerobic granule formation and granule stability in the course of storage and reactor operation. *Biotechnology advances* 28(6), 919-934.
- Ma, H., Chen, Y., Zhu, J., Fan, R., Chen, Z., Meng, L. and Liu, T. 2023. Alleviating the adverse impacts of high influent ammonium on an activated sludge system by adding Fe salts and ballasted media. *Journal of Cleaner Production* 384, 135682.
- Roche, C., Donnaz, S., Murthy, S. and Wett, B. 2022. Biological process architecture in continuous-flow activated sludge by gravimetry: Controlling densified biomass form and function in a hybrid granule–floc process at Dijon WRRF, France. *Water Environment Research* 94(1), e1664.
- Rodriguez-Fabia, S., Torstensen, J., Johansson, L. and Syverud, K. 2022. Hydrophobisation of lignocellulosic materials part I: physical modification. *Cellulose* 29(10), 5375-5393.
- Sang, Y., Lu, T., Lu, X., Wang, S., Shao, X., Han, Y. and Li, L. 2022. Pilot-scale microsand-ballasted flocculation of wastewater: turbidity removal, parameters optimization, and mechanism analysis. *Environmental Science and Pollution Research* 29(21), 32161-32170.

- Wei, S.P., Quoc, B.N., Shapiro, M., Chang, P.H., Calhoun, J. and Winkler, M.K. 2021.
Application of aerobic kenaf granules for biological nutrient removal in a full-scale continuous flow activated sludge system. *Chemosphere* 271, 129522.
- Welling, C.M., Kennedy, A., Wett, B., Johnson, C., Rutherford, B., Baumler, R. and Bott, C. 2015.
Improving settleability and enhancing biological phosphorus removal through the implementation of hydrocyclones. *Proc. Water Environ. Fed.*
- Wett, B., Podmirseg, S., Gómez-Brandón, M., Hell, M., Nyhuis, G., Bott, C. and Murthy, S. 2015.
Expanding DEMON sidestream deammonification technology towards mainstream application. *Water Environment Research* 87(12), 2084-2089.